Clim. Past Discuss., 9, 5227–5261, 2013
www.clim-past-discuss.net/9/5227/2013/
doi:10.5194/cpd-9-5227-2013

Climate of the Past
Discussions
Open Access

Is blue intensity ready to replace maximum latewood density as a strong temperature proxy? A tree-ring case study on Scots pine from northern Sweden

J. A. Björklund[1], B. E. Gunnarson[2], K. Seftigen[1], J. Esper[3], and H. W. Linderholm[1]

[1]Regional Climate Group, Department of Earth Sciences, University of Gothenburg, Gothenburg, Sweden
[2]Bert Bolin Centre for Climate Research, Department of Physical Geography and Quaternary Geology, Stockholm University, Stockholm, Sweden
[3]Department of Geography, Johannes Gutenberg University, Mainz, Germany

Received: 15 August 2013 – Accepted: 29 August 2013 – Published: 10 September 2013

Correspondence to: J. A. Björklund (jesper.bjorklund@gvc.gu.se)

Published by Copernicus Publications on behalf of the European Geosciences Union.

Abstract

At high latitudes, where low temperatures mainly limit tree-growth, measurements of wood density (e.g. Maximum Latewood Density, MXD) using the X-Ray methodology provide a temperature proxy that is superior to that of TRW. Density measurements are however costly and time consuming and have lead to experimentation with optical flatbed scanners to produce Maximum Blue Intensity (BI_{max}). BI_{max} is an excellent proxy for density on annual scale but very limited in skill on centennial scale. Discolouration between samples is limiting BI_{max} where specific brightnesses can have different densities. To overcome this, the new un-exploited parameter Δ blue intensity (ΔBI) was constructed by using the brightness in the earlywood (BI_{EW}) as background, ($BI_{max} - BI_{EW} = \Delta BI$). This parameter was tested on X-Ray material (MXD – earlywood density = ΔMXD) and showed great potential both as a quality control and as a booster of climate signals. Unfortunately since the relationship between grey scale and density is not linear, and between-sample brightness can differ tremendously for similar densities, ΔBI cannot fully match ΔMXD in skill as climate proxy on centennial scale. For ΔBI to stand alone, the range of brightness/density offset must be reduced. Further studies are needed to evaluate this possibility, and solutions might include heavier sample treatment (reflux with chemicals) or image-data treatment (digitally manipulating base-line levels of brightness).

1 Introduction

Various tree-ring parameters provide information on a range of climate parameters with annual resolution. The most commonly used method to extract climate information from trees is the measurement of ring-widths (TRW, e.g. Douglass, 1914). At high latitudes, where low temperatures mainly limit tree-growth, measurements of wood density (e.g. Maximum Latewood Density, MXD) using the X-Ray methodology Schweingruber et al. (1978) provide a temperature proxy that is superior to that of TRW (Wilson and

Luckman, 2003; Grudd, 2008; Esper et al., 2012b; McCarrol et al., 2013). Density measurements are however costly and time consuming, and to robustly represent climate variability on centennial and longer timescales, the number of trees required greatly increases (Esper et al., 2012a) and production rates and costs can become significant obstacles (e.g. Gonzales and Eckstein, 2003).

Recently, an alternative to the X-Ray based density measurements has been developed, that instead utilizes data derived from optical flatbed scanners (see overview in Campbell et al., 2011).

The latest efforts in developing this technique have focused on the reflected light in the blue spectrum, and using young silvicultured Scots pine from Northern Finland it was shown that minimum Blue Intensity (BI_{min}) and MXD are highly correlated on annual to decadal scales (McCarrol et al., 2002; Campbell et al., 2007). Blue Intensity has subsequently been considered to be a potential surrogate for MXD. In an effort to make the proxy more available to researchers, Campbell et al. (2011) published an applications manual where a standard protocol was recommended. However, it can be argued that rather than using the Campbell et al. (2011) standard protocol, where BI_{min} is analysed, the blue light intensity scale should be inverted as is traditionally done with the X-Ray grey scale. We feel that this will simplify the nomenclature and propose that maximum blue intensity (BI_{max}) rather than BI_{min} should be used, as it is a more intuitive counterpart to the MXD parameter. This will be done throughout this paper.

In McCarrol et al. (2013) the first millennial long BI_{max} chronology was presented. The chronology was developed from Scots pine from Khibiny, on the Kola Peninsula in Russia. The chronology was shown to be an excellent proxy for summer temperatures, comparable to the Finnish, Swedish and Norwegian MXD chronologies in the same study. However, long timescales were filtered out of the Khibiny BI_{max} chronology with traditional tree-ring standardisation techniques (Cook, 1985), as a consequence of the "segment length curse" (Cook et al., 1995). Thus the validity of the chronology could only be evaluated on shorter timescales, and still no study has to date shown that BI_{max} versus MXD relationship holds on multi-centennial and longer time-scales.

CPD
9, 5227–5261, 2013

1.1 X-Ray and blue intensity techniques

The X-Ray density method relies on measuring residual X-Ray radiation beamed through a tree-sample of known depth. The residual X-Ray radiation is captured as an inverted grey scale image. Performing the same procedure with a "standard" of known depth *and* density enables calculations of all grey levels in the sample-image into density. Tracking the density profile in the image with regard to tree-age the MXD measurement is the peak value in the latewood each year (Fig. 1). Likewise, measurements of earlywood density (ED) can be calculated as the mean density over the earlywood width (see Helama et al., 2008 for an overview of density and ring width parameters). The "standard" used for calibration of X-Ray grey levels into wood density is commonly a calibration wedge made out of cellulose acetate (Schweingruber et al., 1988), a compound with properties similar to lignin, which is the material that lends the plant cell wall compressive strength and stiffness (Raven et al., 2004). The X-Ray grey levels can thus be transformed into lignin content or wood density. The lignin content in the wood can be interpreted as an estimate of favourable or unfavourable conditions (Gindl et al., 2000), and for trees growing in cool temperate regions, warm growing seasons are favourable and connected to dense/dark MXD while cool summers are unfavourable and related to transparent/bright MXD.

The Blue Intensity technique is analogously based on radiation but in the visible blue light spectrum. Here the blue light that is reflected is captured in grey scale images. Scanned images can similarly to X-Ray images be analysed in commercial image analysis soft wares e.g. Windendro (Guay et al., 1992) or Coorecorder (www.cybis.se). As with X-Ray images of wood samples and associated wood "density profiles" (Fig. 1), the scanned images can also be described with "colour profiles" (second *y* axis in Fig. 1, note that sample image in the figure is an X-Ray image, but in principle the scanned image looks the similar). The scanned images are analogue to the X-Ray images but are merely a reflection of the wood colour of the surface (2-D) while X-Ray images are measures of the wood in a volume (3-D). Consequently, scanned measurements are only proxies for density while X-Ray measurements are true measures of density after calibration and thus associated with greater reliability. Previous blue intensity studies have not attempted to transform blue intensity values into density, which is standard procedure in the X-Ray technique. The relationship between X-Ray grey levels and density is non-linear and describes roughly an exponential increase of wood density with linear increase in grey level (Fig. 2a). Likewise a linear relationship between blue intensity and density is not expected and consequently if a direct comparison between MXD and BI_{max} is going to be made, BI_{max} must also be transformed into density.

Unfortunately, since the blue intensity method is only a 2-D measure, slight discolorations of the wood can be critical when transforming blue colour into wood density. One obvious source of uncertainty with BI_{max} is that many coniferous tree-species have their woody tissue divided into heartwood and sapwood (Sheppard et al., 1996). The heartwood does not contain living cells and is not active in transport as opposed to the sapwood. The colour of heartwood and sapwood differs and is often a result of differential allocation of oils, gums, resins and tannins to the heartwood discolouring the wood (Raven et al., 2004). As heartwood and sapwood have sometimes very different colour, but not very different densities, there is a risk of potential offset in light measurements versus density transgressing this boundary. Another question is if the colour *between* wood samples within a species is as homogenous as the densities are? There might even be an age/preservation related bias in colour between samples/trees. When transforming BI_{max} into a climate reconstruction it is vital that blue light values relationship to density is constant. If specific blue light values can be associated with different densities and opposite, a climate reconstruction will be seriously flawed.

1.2 Objectives

Here we present and analyse a new, highly replicated multi-generation > 800 yr long Scots pine (*Pinus Sylvestris* L.) chronology from northern Fennoscandia. Both X-Rayed and scanned measurements were made on the *same* cores to directly evaluate the relationship between MXD and BI_{max}. This study aims to evaluate the relationship be-

CPD
9, 5227–5261, 2013

tween BI_{max} and MXD over several generations of trees, which has never been attempted before. A new approach meant to remedy the brightness/density bias when transgressing the heartwood/sapwood boundary or between-sample brightness is introduced. This method relies on the assumption that the earlywood and latewood of the same year is discoloured consistently and a difference between BI_{max} and mean earlywood blue intensity (BI_{EW}) is calculated to give the latewood measurement a baseline and become colour independent, ($BI_{max} - BI_{EW}$) here termed ΔBI (Fig. 1). This exercise was considered in another form (as a ratio between latewood and early wood brightness) by Sheppard et al. (1996) and was described as a harsh statistical treatment by McCarrol et al. (2002). Here we show that also removing the ED from MXD, yielding ΔMXD, has its merits by testing it on a selection of the finest MXD chronologies in Fennoscandia. We also show that this can work as a quality control and clean up climate signals when using the X-Ray technique.

2 Data and methods

2.1 Study area

A site in Northern Sweden, 50 km north of the town of Arjeplog at 66°2′ N and 18°1′ E, was sampled for Scots Pine (*Pinus Sylvestris* L.) (Fig. 3). The source area for the sampled trees is a north-facing slope of a mountain reaching an elevation of 800 m, where pines, together with sparse Downy birch (*Betula pubescens* Ehrh), form the tree-line at 700 m a.s.l. The sampling strategy for the Arjeplog chronology was to target a range of ages of living trees from as young as 10 yr old to as old as possible, and *all* dead material that could be found in the sampled area. All trees were collected between 500 m a.s.l and the tree line. The forest is a patchwork of dense Norway spruce – *Picea abies* (L.) Karst – stands in wetter pockets and sparse Scots pine stands on drier better-drained blocky terrain. In the wetter terrain there are also substantial inclusions of Downy birch. In the Pine stands snags are abundant. The climate in the area is

CPD
9, 5227–5261, 2013

cool and temperate with mean monthly temperatures ranging from $-14\,^{\circ}\mathrm{C}$ in January to $13\,^{\circ}\mathrm{C}$ in July and a mean annual precipitation of 553 mm, recorded at Arjeplog meteorological station 1961–1990, (data from the Swedish Meteorological and Hydrological Institute).

2.2 Tree-ring data

In this comparative case study, the same tree-core samples were both X-Rayed and scanned. 250 trees were sampled and dated and out of these 140 were selected for further analysis. It is important to note that it was not entirely the same "tracks" that were measured on the wood samples even though the same cores were measured. This may have minor effects on single measurement series, so the mean chronologies were not expected to be entirely identical. The X-Rayed data was produced using an ITRAX multiscanner from Cox Analytical Systems (www.coxsys.se). The samples were prepared according to standard dendrochronological techniques (Schweingruber et al., 1978). Thin laths were cut from the samples using a twin-bladed circular saw (1.20 mm thick) and treated with alcohol in a Soxhlet apparatus in order to extract resins and other soluble compounds. The laths were X-Rayed with 12 % water content (air dry). The ITRAX multiscanner was equipped with a chrome tube, tuned at 30 Kv and 50 mA, and the samples were X-Rayed with a narrow, high energy, X-Ray beam in steps of 20 µm with 75 mS step time. For each step a sensor with a slit opening of 20 µm registered residual radiation that was not absorbed by the sample. The multiscanner produces an 8-16 bit, inverted grey scale digital image at 1.270 dpi resolution. Calibration of the grey scale was done with a calibration wedge of cellulose acetate with a density of $1.274\,\mathrm{g\,cm^{-3}}$ (Schweingruber et al., 1988).

The scanned data was produced using the standard protocol according to Campbell et al. (2011). The remaining wood pieces, after twin-blading the laths for X-Ray analysis, was sanded with increasingly finer grit sandpaper, with 600-grit paper the final round. The samples were then refluxed in a soxhlet apparatus with alcohol (~24 h, roughly 15 cycles, same as for the X-Ray laths). A final touch-up with the fine grit

CPD
9, 5227–5261, 2013

sandpaper was made after reflux to again fill all fibre voids with wood dust. This was done to enhance contrast in the samples, and also to avoid patchy samples (occasionally empty fibre voids found next to filled fibre voids). A visual inspection of resin content was made to ensure that all obvious resin pockets were removed. The digital images were produced with a flatbed Scanner at 1600 dpi resolution (Epson Perfection V600 Series) calibrated with SilverFast Ai professional scan software using the IT8 Calibration Target (IT8.7/2). All images, X-Rayed and scanned, were analysed in the commercial software WinDendro™.

Contrary to the Campbell et al. (2011) standard protocol, the blue light intensity data produced in this study was inverted (Fig. 2b) as is traditionally done in the X-Ray method. The blue light levels were analysed both with and without calibration into wood density. Since there is no "standard" for calibrating blue light into density, like with the X-Ray calibration wedge, calibration of scanned measurements against the X-Ray measurements had to be made. The relationship between measurements was established by fitting an ordinary least square (OLS) exponential regression line between the X-Ray and scanned data. The non-linear relationship between X-Ray image grey levels and density is roughly describing an exponential increase in density with linear increase in grey level. Therefore, exponential fits were chosen to represent OLS fits between X-Ray densities and scanned blue light intensity. Sample-specific exponential OLS fits were used to calibrate the scanned data individually (Fig. 4c, left panel), and alternatively, one mean exponential function for the scanned data as a group (Fig. 4d, left panel). The entire X-Ray dataset was sorted from low to high values with corresponding blue intensity values. A running mean of the two datasets were calculated for every 5000 data points with an overlap of 2500 data points. These new running mean points were then regressed against one another and an OLS exponential function was calculated and used for calibration of the entire blue intensity dataset (Fig. 4d, left panel).

CPD
9, 5227–5261, 2013

2.3 Tree-ring reference data

To further evaluate the new data and methods, three X-Ray reference chronologies were used (Fig. 3): N-Scan (Esper et al., 2012b); Forfjorddalen (McCarrol et al., 2013) and Jämtland (Gunnarson et al., 2011). These three chronologies neighbour Arjeplog with Jämtland in the South, N-Scan in the northeast and Forfjorddalen in northwest. Forfjorddalen and Jämtland were analysed with the ITRAX system while N-Scan was analysed using the Walesch system (see Esper et al., 2012b). The Walesch system is an analogue technique, in which the laths are placed on X-Ray film and exposed to X-Rays. The film will have much higher resolution than the digital image produced with the ITRAX multi scanner. The grey-level intensity in the film is converted to absolute density values using a manually operated photo-sensor with the aid of a calibration wedge (Schweingruber et al., 1988).

2.4 Climate data

In order to identify and evaluate climate signals in the X-Rayed data from Arjeplog and the three reference chronologies, a response analysis to instrumental temperature data was made using the DENDROCLIM2002 software (Biondi and Waikul, 2004). The 1° gridded mean land temperature CRUTS3.1 dataset (Harris et al., 2013) was used, where the chronologies were compared against the closest respective grid-point temperature. The common overlap between the chronologies and observational data was 1901–2006 and used in all climate response analyses. The response analysis was made using first differenced proxy and instrumental data. This process removes all variation on the medium and low frequency bands to prevent biased correlations due to spurious similarities in trends (cf. Cook et al., 1990).

CPD
9, 5227–5261, 2013

2.5 Comparative analyses

A simple set of comparative analyses was utilized in this study. Pearson correlation coefficients were calculated among all tree-ring datasets and were also performed with first differenced data. Plotting of chronologies together with residuals was used to facilitate comparison of the lower frequencies. Chronology confidence was evaluated using the expressed population signals (EPS; Wigley et al., 1984). The EPS represents the percentage of the variance in a hypothetical population accounted for by the sample, here calculated for 50-yr moving windows with a 25-yr lag. A value above 0.85 is generally considered adequate (Wigley et al., 1984).

Frequency distributions of mean earlywood and maximum latewood values from all raw X-Rayed and scanned chronology data points were made to visualize differences and similarities in the datasets. Relationships between MXD, ED and ΔMXD as well as BI_{max}, BI_{EW} and ΔBI were also plotted and compared together in chronology format (see parameter definition in Fig. 1). The blue light levels were adjusted to reflect/represent roughly the same interval as the mean level of the X-Ray measurements. All chronologies were compared and analysed raw, that is, not transformed into indices by standardisation, except for the comparison of the MXD versus ΔMXD reference chronologies. These MXD and ΔMXD chronologies were standardised using Regional Curve Standardisation (RCS; Briffa et al., 1992; Cook and Krusic, 2005) to remove age related trends in the series. RCS was used to enable comparison of chronologies on longer time scales and to exclude possible age-class bias through time between the chronologies (Cook et al., 1995).

2.6 Δ maximum latewood density and Δ blue intensity, two previously unexploited proxies

If untreated with alcohol, the heartwood and sapwood will have very different colours (Fig. 5a), and this colour difference is reduced but not removed after ethanol reflux (Fig. 5a). Not removing the colour difference entirely will cause an offset in the blue light measurements compared to the X-Ray measurements at the transgression boundary, and there was also an even more pronounced difference in colour *between* the refluxed samples (Fig. 5b). To test the differential discolouration between samples for systematic biases, tree brightness averages and standard deviations were regressed against calendar date of the last measured heartwood ring. The discoloration within an annual ring was however hypothesized to be similar in latewood and earlywood. This assumption enabled a correction of ambient discoloration by simply subtracting mean earlywood measurements from maximum latewood measurements, resulting in the previously unexploited parameters: ΔMXD or ΔBI (Fig. 1). The earlywood values provide a baseline for the more dominant signal carrier MXD or BI_{max}. The method was tested on the X-Rayed reference data in regard to climate sensitivity and annual to centennial scale variability in line plots. The hypothesis was that if ΔMXD has equally robust and rational climate signal as MXD, the method could also be used to produce unbiased ΔBI. The ΔBI was then compared to ΔMXD in line plots and checked for drift in residuals.

3 Results

The MXD and BI_{max} chronologies have sufficient EPS values for the entire analysed period, except for one segment around 1600 AD. The first differenced MXD and BI_{max} chronologies have a correlation of $r = 0.95$, and the ΔMXD and ΔBI a correlation of $r = 0.97$ ($n = 810$). Examining the common variability visually on longer timescales, the MXD and BI_{max} co-vary excellently from 1200 AD to 1700 AD (Fig. 6, note that all chronologies were z scored using this period). After this, there is a dramatic divergence between the MXD and BI_{max}. This negative trend in BI_{max} is also seen in Fig. 7b where BI_{max} and BI_{EW} are combined as sample-mean and standard deviation. Here it can also be seen that MXD together with ED also has a negative trend (Fig. 7a). To overcome the possible systematic bias of brightness levels in the latewood, the ΔBI parameter was used. This new parameter was tested on X-Rayed material, MXD versus ΔMXD, with regard to its climate signal. Examining the reference chronologies, the MXD showed positive and significant ($p < 0.05$) responses to April through August temperatures for almost all sites, except in June for Forfjorddalen (Fig. 8). ED also responds positive to April–May temperatures but negative to June and July. ΔMXD had on average no significant response to April and low but significant response to May and a strong June-August response. The JJA signal strengths in the chronologies over 1901-2006 are: N-scan ($r^2_{MXD} = 0.53$, $r^2_{\Delta MXD} = 0.66$); Forfjorddalen ($r^2_{MXD} = 0.47$, $r^2_{\Delta MXD} = 0.61$); Jämtland ($r^2_{MXD} = 0.51$, $r^2_{\Delta MXD} = 0.65$) and Arjeplog ($r^2_{MXD} = 0.50$, $r^2_{\Delta MXD} = 0.58$) see also Table 1.

The MXD and ΔMXD are very similar in all frequencies for all reference chronologies but there is a slight difference in overall trend in the Arjeplog chronology (Fig. 9).

The expected distribution of density data points using X-Ray density as standard would be a small range of ED values clustering around 350–400 g dm^{-3} and a larger range for MXD clustering around 650 g dm^{-3} (Fig. 4a) with little overlap between ED and MXD values. This distribution was not found in the non-calibrated BI_{EW} and BI_{max} values. Instead, their distributions were similar to each other with a large overlap (Fig. 4b). The standard deviations were very small compared to the X-Ray counterparts. BI_{max} have 50 % larger standard deviations than BI_{EW}, whereas MXD has double the standard deviation compared to ED (Fig. 4a and b, right panel). Overall trends in BI_{EW} and BI_{max} are steeply negative (Fig. 4b). However, if all blue data were calibrated individually with the X-Ray data, the two datasets could not be separated in any respect (Figs. 4c and 10b). All individual exponential functions are plotted together in the left panel in Fig. 4c and there is large scatter of functions, but the shape or curvatures of the functions are roughly similar (Fig. 4c). Using one mean exponential function for all blue light data series, the distributions of data point can be described as mixture of the X-Ray data distribution and the non-calibrated blue light data distribution (Fig. 4d). Standard deviations are same as for the X-Ray data but the steep negative trends in BI_{max} and BI_{EW} return.

CPD
9, 5227–5261, 2013

The result of the different calibrations on the blue intensity data can be seen in Fig. 10a–c, where ΔBI is compared to ΔMXD. Not applying calibration into density lead to a clearly positively biased ΔBI chronology (Fig. 10a), while calibration with individual functions gives no overall trend in residuals (Fig. 10b) but they are by no means random, and calibrating with one mean function leads to a negatively biased ΔBI chronology (Fig. 10c).

4 Discussion

Sampling around 250 trees, living and dead, would ideally yield quite homogenous replication through time with fewer dating-counts going back in time. This was however not the case at Arjeplog where the chronology in general has a high replication except for around the 1600s when the replication is very low, 9 trees minimum (Fig. 6). The reason for this is probably that a majority of the older generation of trees has died back and given favourable seedling conditions, a so-called regeneration (Zackrisson et al., 1995) around 1700 AD. The snag material, dead fallen trees preserved on the ground, lacked sapwood in almost all cases (see Fig. 6 for sapwood heartwood distribution through time). If the sapwood had not been decomposed in the older samples, the depression in replication in the 1600s would likely not exist. The EPS drops under or close to the threshold of 0.85 for chronology confidence around this period. This is of course negative for the analysis but not critical since the drop in replication is identical in both the X-Rayed and scanned datasets.

The level of correlation between MXD and BI_{max} and ΔMXD and ΔBI is so high that it would hypothetically be very difficult to distinguish from a correlation between two MXD chronologies made on the same material but by two different investigators. Thus it is again corroborated that BI_{max} is an excellent proxy for *relative* density from MXD in wood. However, when it comes to the long-timescale variations, it is clear that BI_{max} is not capable of representing absolute density values since specific BI_{max} values can be associated with different densities (Fig. 6). The 300-yr divergence between MXD and

BI_{max} is not only a product of the heartwood/sapwood difference in blue intensity but is probably mainly a result of the difference in discolouration among samples. Figure 7b show the mean and standard deviation of BI_{max} together with BI_{EW} heartwood material regressed against time, and it is clear that modern or living-tree samples are on average brighter than the older snag material (Fig. 5b). Note that this analysis was made without sapwood material. We offer no explanation to the trend in blue intensity but suspect that longer residence time of oils, gums, resins and tannins in the wood, likely result in a more permanent discolouration. We conclude that there is a systematic bias in the colour of at least this sample population that has some kind of age component in it. Better methods to remove these compounds are therefore of great importance, and longer treatment times for older material should perhaps be considered in future work. A time dependent systematic drift towards lower MXD and ED is also indicated in Fig. 7a, but here standard deviations are two times larger on average and the chronology trend becomes small as seen in Fig. 6. To be able to use blue intensity as climate proxy this systematic bias must be removed, and an attempt to do this is to transform BI_{max} into ΔBI using the BI_{EW} as background.

4.1 Validation of the Δ parameter using X-Ray data

The climate responses of the four MXD chronologies to April-August temperatures are consistent with many other studies on MXD from the region (e.g. Briffa et al., 2001; Björklund et al., 2013). McCarroll et al. (2003) suggest that MXD represents a proxy measure of net photosynthesis over the entire growing season. To include April in the growing season might seem unlikely since mean temperatures are below 0 °C, but Salminen and Jalkanen (2007) reports apical cambial activity in Scots pine on these latitudes around the end of April, which is arguably why also temperatures in this month can be tied to wood density.

The less investigated parameter ED showed positive response to April and May temperature but a negative response in July. The highest growth rates of the cells in Scots pine on these latitudes occur in July (Hustich, 1956; Schmitt et al., 2004; Seo et al.,

CPD
9, 5227–5261, 2013

2008), so our interpretation is that if July is warm, large cells are produced that lead to less dense wood. Lignification of the cell wall completes the maturation of a tracheid and follows just after cell formation (Wight, 1933; Gindl et al., 2000). Gindl et al. (2000) reported that favourable conditions give more lignification and we interpret this so that a warm April–May likely provides more photosynthetic assimilates and as result higher lignin content in the cell walls. Consequently, the earlywood cell walls would become thicker and the earlywood denser.

ED and MXD seem to share the positive spring response. If the lignification is considered as total collection of assimilates during the growing season the response would likely be similar in ED and MXD, but ED only responds to spring while MXD responds to both spring and summer. The MXD measurement is thus intra-seasonally auto correlated with ED. Subtracting the earlywood measurement from the maximum latewood measurement would thus weaken the April–May ΔMXD signal, which is also observed (Fig. 8). The different response to July in ED and MXD is likely related to that ED is more cell-size dependent while MXD is more cell-wall thickness dependent. The ΔMXD parameter response to July becomes purified from the cell size variation and early season lignification, and the summer climate response is boosted. We argue that a shorter and later summer temperature signal therefore can be extracted from ΔMXD. However, the MXD and ΔMXD still share most of their variation, equivalently an April–August temperature mean share most of the information with a June–August temperature mean, and we therefore anticipate that MXD and ΔMXD are very similar on all timescales, and even more so on longer timescales. This is supported by that the N-Scan, Forfjorddalen and Jämtland ΔMXD chronologies are almost identical to their MXD counterparts (Fig. 9). However, in the Arjeplog chronology there is a visible drift between the MXD and ΔMXD chronologies although the annual variability is almost identical (Fig. 9a). As suggested earlier, this is likely a sign of biased X-Ray measurements where oils, gums, resins and tannins have had a significant influence also on the wood density. Using ED to calculate ΔMXD could thus in this way act as a quality control for MXD. An agreeable side effect of using ΔMXD seems to be that the June–

CPD
9, 5227–5261, 2013

August signal is boosted. In conclusion, the ΔMXD or ΔBI parameter clearly contain plausible information, and can be used for further analyses of Blue Intensity data.

4.2 ΔBI, a complement to MXD?

The overlap between the MXD and ED data distributions (Fig. 4a, middle panel), would probably be smaller if the X-Ray density produced for this study would be less biased by non-lignin induced density levels. However we have no reason to suspect that the samples were refluxed for too short time in this study, because trials of longer residence times (7 days) of three samples in alcohol, acetone and Hydrogen peroxide did not yield a measurable change in colour levels. These tentative trials were made as a reaction to the biased density measurements. Instead, we speculate that snags with relatively little incorporation of oils, gums, resins and tannins, are more readily decomposed and consequently only the most discoloured snags were to be found.

The bias in brightness with time is overwhelming in the non-calibrated blue light material (Fig. 4b) where BI_{max} values are frequently occupying the same level of magnitudes as the BI_{EW}. Their respective chronology describe roughly similar trends and the older BI_{EW} data cannot be separated in brightness level from modern BI_{max} data. The blue intensity data, in this study, is again clearly shown *not* to be a proxy for absolute density. What it does indicate however, is that the earlywood and latewood seem to be similarly discoloured, which is why ΔBI appears to be a promising solution.

Calibrating each scanned pair of BI_{max} and BI_{EW} against their counterpart pair MXD and ED gives very good results when it comes to likeness in variance of individual series. The ΔBI – ΔMXD residuals are small with no overall trend (Fig. 10b). But all this shows is that if the older and more modern samples would have had more similar mean colour, ΔBI could be used as proxy for absolute density change from early wood to maximum latewood levels. This was however not the case and is highlighted by the test with one calibration function for all blue data. This function is doing a fair job, but overall it inflates high blue intensity values and compresses low values too much (Fig. 11b, grey circles). The difference in inflation and compression is distorting the counteracting

CPD
9, 5227–5261, 2013

trends in BI_{max} and BI_{EW} against each other, and the resulting ΔBI chronology will have a negatively biased trend: note the different slopes in Fig. 11a–c where calibration give much more negative slope than no calibration. Figure 11 is only made on two series but aims to illustrate the relationship between older series and modern series, that variance manipulation will distort resulting ΔBI trends. The distortion in the ΔBI chronology that use one calibration function for blue measurements (Fig. 10c) is not large but would still be critical to a climate reconstruction.

With less curvature in the calibration function the ΔBI chronology distortion will be positive and more curvature will lead to negative chronology distortion. This means that there is a middle-ground curvature that will produce ostensibly adequate coherence between ΔBI and ΔMXD but individual series will still be biased in variance. The goodness of fit is achieved by chance when the differences in BI_{EW} and BI_{max} trends match the difference in ED and MXD trends. An acceptable ΔBI chronology can only be achieved when between-sample discolouration is reduced. The critical obstacle in trying to create a high-quality climate reconstruction from blue intensity is not the heartwood/sapwood transition but the differential discoloration between wood samples. Since it is the relation between earlywood and maximum latewood parameters that is of interest, not absolute values, all samples in a study could be washed, bleached or coloured to a similar baseline nuance and used to create unbiased ΔBI chronologies. Granted that the samples in this study were not biased in MXD, and more like the "reference chronologies", hypothetically the ΔBI might not have been biased. Further studies are needed to test these hypotheses. However, attempting to make unbiased BI_{max} chronologies using baseline methods would be almost impossible since it is very difficult to know when the washing, bleaching or colouration have produced perfect levels and even then the heartwood/sapwood problem still remain.

CPD
9, 5227–5261, 2013

5 Conclusions

Our results showed that ΔMXD is an attractive alternative or complement to MXD if a shorter target season is required or as a quality control of the MXD measurements. Moreover, blue light intensity from trees can be utilized as an excellent surrogate for *relative* X-Ray density. It is however a complex matter to fully capture the density levels in a corresponding MXD chronology because specific blue light intensity values obviously can be associated with a range of different density values. Constructing ΔBI and comparing it with ΔMXD will reduce chronology differences dramatically as opposed to BI_{max} compared to MXD. But for ΔBI to stand alone, the range of brightness/density offset must be reduced. Further studies are needed to evaluate this possibility, and solutions might include heavier sample treatment (reflux with chemicals) or image-data treatment (digitally manipulating base-line levels of brightness). Provided that this works, ΔBI can be used as reliable climate proxy for multi-centennial scale climate reconstructions. Since Blue light intensity is so much more inexpensive than the X-Ray counterpart it could in the future be used to drastically improve spatial distribution and replication in highly climate sensitive tree-ring chronologies and lead to higher confidence in climate reconstructions.

Acknowledgements. We thank the PAGES organisation for the opportunity of publishing in YSM2 special issue of Climate of the Past. We also thank Kenth Björk (Skogsstyrelsen Administrator Arjeplogs common land) for valuable advice and permission to collect the Arjeplog tree-ring chronology. This work was supported by Vetenskapsrådet and Formas (grants to Hans W. Linderholm). The paper contributes to the Swedish strategic research areas Modelling the Regional and Global Earth system (MERGE), and Biodiversity and Ecosystem services in a Changing Climate (BECC). This is contribution #24 from the Sino–Swedish Centre for Tree ring Research (SISTRR).

CPD
9, 5227–5261, 2013

References

Biondi, F. and Waikul, K.: DENDROCLIM2002: a C++ program for statistical calibration of climate signals in tree-ring chronologies, Comput. Geosci., 30, 303–311, 2004.

Björklund, J. A., Gunnarson, B., Krusic, P., Grudd, H., Josefsson, T., Östlund, L., and Linderholm, H.: Advances towards improved low-frequency tree-ring reconstructions, using an updated Pinus sylvestris L. MXD network from the Scandinavian Mountains, Theor. Appl. Climatol., 113, 697–710, 2013.

Briffa, K. R., Jones, P. D., Bartholin, T. S., Eckstein, D., Schweingruber, F. H., Karlén, W., Zetterberg, P., and Eronen, M.: Fennoscandian summers from AD 500: temperature changes on short and long time scales, Clim. Dynam., 7, 111–119, 1992.

Briffa, K. R., Osborn, T. J., Schweingruber, F. H., Harris, I. C., Jones, P. D., Shiyatov, S. G., and Vaganov, E. A.: Low-frequency temperature variations from a northern tree-ring density network, J. Geophys. Res., 106, 2929–2941, 2001.

Campbell, R., McCarroll, D., Loader, N. J., Grudd, H., Robertson, I., and Jalkanen, R.: Blue intensity in *Pinus sylvestris* tree-rings: developing a new palaeoclimate proxy, Holocene, 17, 821–828, doi:10.1177/0959683607080523, 2007.

Campbell, R., McCarroll, D., Robertson, I., Loader, N. J., Grudd, H., and Gunnarson, B.: Blue Intensity in Pinus Sylvestris tree-rings: A manual for a new palaeoclimate proxy, Tree-Ring Res., 67, 127–134, 2011.

Cook, E. R.: A time series analysis approach to tree ring standardization, Dissertation, University of Arizona, 1985.

Cook, E. R. and Kairiukstis, L. A. (Eds.): Methods of Dendrochronology: Applications in The Environmental Sciences, Kluwer Academic Publishers, Dordrecht, 394 pp., 1989.

Cook, E. R. and Krusic, P. J.: Program ARSTAN, A tree-ring standardization program based on detrending and autoregressive time series modeling with interactive graphics. Tree-Ring Laboratory, Lamont-Doherty Earth Observatory, Columbia University, Palisades, NY, 2005.

Cook, E. R., Briffa, K. R., Meko, D. M., Graybill, D. A., and Funkhouser, G.: The "segment length curse" in long tree-ring chronology development for palaeoclimatic studies, Holocene, 5, 229–237, 1995.

Douglass, A. E.: Method of estimating rainfall by the growth of trees, B. Am. Geogr. Soc., 46, New York, 1914.

CPD
9, 5227–5261, 2013

Esper, J., Büntgen, U., Timonen, M. and Frank, D. C.: Variability and extremes of Northern Scandinavian summer temperatures over the past millennia, Global Planet. Change 1, 88–89, 2012a.

Esper, J., Frank, D. C., Timonen, M., Zorita, E., Wilson, R. J. S., Luterbacher, J., Holzkämper, S., Fischer, N., Wagner, S., Nievergelt, D., Verstege, A., and Büntgen, U.: Orbital forcing of tree-ring data, Nat. Clim. Change, 2, 862–866, doi:10-1038/NCLIMATE1589, 2012b.

Gindl, W., Grabner, M., and Wimmer, R.: The influence of temperature on latewood lignin content in treeline Norway spruce compared with maximum density and ring width, Trees – Struct. Func., 14, 409–14, 2000.

González, I. G. and Eckstein, D.: Climatic signal of early wood vessels of oak on a maritime site, Tree Physiol., 23, 497–504, 2003.

Grudd, H.: Torneträsk tree-ring width and density AD 500–2004: a test of climatic sensitivity and a new 1500-year reconstruction of north Fennoscandian summers, Clim. Dynam., 31, 843–857, 2008.

Guay, R., Gagnon, R., and Morin, H.: A new automatic and interactive tree measurement system based on a line scan camera, Forest Chron., 68, 138–141, 1992.

Gunnarson, B. E., Linderholm, H. W., and Moberg, A.: Improving a tree-ring reconstruction from west-central Scandinavia — 900 years of warm-season temperatures, Clim, Dynam., 36, 97–108, 2011.

Harris, I., Jones, P. D., Osborn, T. J., and Lister, D. H.: Updated high-resolution grids of monthly climatic observations, Int. J. Climatol., doi:10.1002/joc.3711, in press, 2013.

Helama, S., Vartiainen, M., Kolström, T., Peltola, H., and Meriläinen, J.: X-Ray microdensitometry applied to subfossil tree-rings: growth characteristics of ancient pines from the southern boreal forest zone in Finland at intra-annual to centennial time-scales, Veg. Hist. Archaeobot., 17, 675–686, doi:10.1007/s00334-008-0147-9, 2008.

Hustich, I.: Notes on the growth of Scotch pine in Utsjoki in northernmost Finland, Acta Bot. Fenn., 56, 1–13, 1956.

McCarroll, D., Pettigrew, E., Luckman, A., Guibal, F., and Edouard, J. L.: Blue reflectance provides a surrogate for latewood density of high-latitude pine tree-rings, Arct. Antarct. Alpine Res. 34, 450–53, 2002.

McCarroll, D., Jalkanen, R., Hicks, S., Tuovinen, M., Gagen, M., Pawellek, F., Eckstein, D., Schmitt, U., Autio, J., and Heikkinen, O.: Multiproxy dendroclimatology: a pilot study in northern Finland, Holocene, 13, 829–838, 2003.

McCarroll, D., Loader, N. J., Jalkanen, R., Gagen, M. H., Grudd, H., Gunnarson, B. E., Kirchhefer, A. J., Friedrich, M., Linderholm, H. W., Lindholm, M., Boettger, T., Los, S. O., Remmele, S., Kononov, Y. M., Yamazaki, Y. H., Young, G. H. F., and Zorita, E.: A 1200-year multiproxy record of tree growth and summer temperature at the northern pine forest limit of Europe, Holocene, 23, 471–484, doi:10.1177/0959683612467483, 2013.

Raven, P. H.: Biology of Plants, Sixth Edition, WH Freeman and Company/Worth Publishers, USA, 1999.

Salminen, H. and Jalkanen, R.: Intra-annual height increment of Pinus sylvestris at high latitudes in Finland, Tree Physiol., 27, 1347–1353, 2007.

Schmitt, U., Jalkanen, R., and Eckstein, D.: Cambium dynamics of *Pinus sylvestris* and *Betula* spp. in the northern boreal forest in Finland, Silva Fenn., 38, 167–178, 2004.

Schweingruber, F. H., Fritts, H. C., Bräker, O. U., Drew, L. G., and Schär, E.: The X-Ray technique as applied to dendrochronology, Tree-Ring Bull., 38, 61–91, 1978.

Schweingruber, F. H., Bartholin, T., Schär, E., and Briffa, K. R.: Radio-densitometric dendroclimatological conifer chronologies from Lapland (Scandinavia) and the Alps (Switzerland), Boreas, 17, 559–566, 1988.

Seo, J.-W., Eckstein, D., Jalkanen, R., Rickebusch, S., and Schmitt, U.: Estimating the onset of cambial activity in Scots pine in northern Finland by means of the heat-sum approach, Tree Physiol., 28, 105–112, 2008.

Sheppard, P. R., Graumlich, L. J., and Conkey, L. E.: Reflected-light image analysis of conifer tree-rings for reconstructing climate, Holocene, 6, 62–68, doi:10.1177/095968369600600107, 1996.

Wight, W.: Radial growth of the xylem and the starch reserves of Pinus Sylvestris: A preliminary Survey, New Phytol., 32, 77–96, doi:10.1111/j.1469-8137.1933.tb07000.x, 1933.

Wigley, T. M. L., Briffa, K. R., and Jones, P. D.: On the average value of correlated time series, with applications in dendroclimatology and hydrometeorology, J. Clim. Appl. Meteorol., 23, 201–213, 1984.

Wilson, R. J. S. and Luckman, B. H.: Dendroclimatic reconstruction of maximum summer temperatures from upper treeline sites in Interior British Columbia, Canada, Holocene, 13, 851–861, 2003.

Zackrisson, O. M., Nilsson, C., Steijlen, I., and Hörnberg, G.: Regeneration pulses and climate-vegetation interactions in nonpyrogenic boreal Scots pine stands, J. Ecol., 83, 469–483, 1995.

Table 1. Explained variance in JJA temperatures from MXD and ΔMXD as well as BI_{max} and ΔBI. Temperature data from CRUTS3.1 dataset (Harris et al., 2013).

Chronology	R^2 MXD vs. JJA Temp.	R^2 ΔMXD vs. JJA Temp.
Arjeplog	0.50	0.59
Forfjorddalen	0.47	0.61
Jämtland	0.51	0.65
N-Scan	0.53	0.66
	R^2 BI_{max} vs. JJA Temp.	R^2 ΔBI vs. JJA Temp.
Arjeplog	0.54	0.62

CPD
9, 5227–5261, 2013

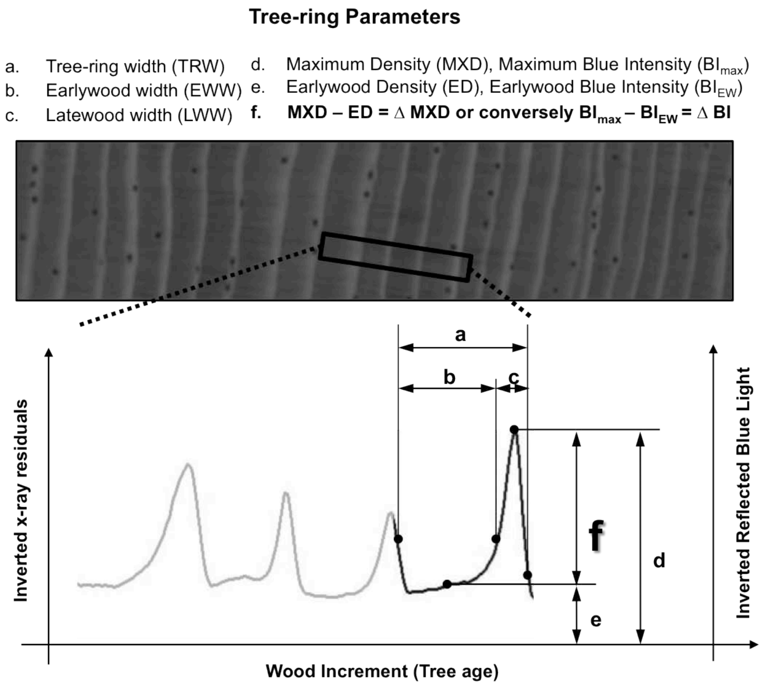

Fig. 1. Schematic of different tree-ring parameters to show the relation of new previously unexploited ΔMXD and ΔBI with other more familiar ones. Note that the blue intensity parameters are using the X-Ray image, which is essentially similar to a scanned image.

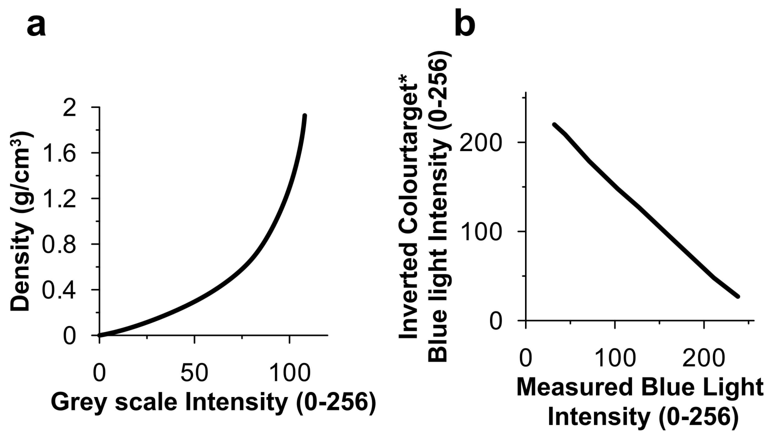

Fig. 2. (a) Schematic diagram over the relationship between wood density and X-Ray image grey scale intensity. **(b)** Schematic diagram over the inverted relationship between colour target IT8/7 and measured blue light intensity in WinDendro, used in this study.

CPD
9, 5227–5261, 2013

Is Blue Intensity ready to replace Maximum Latewood Density?

J. A. Björklund et al.

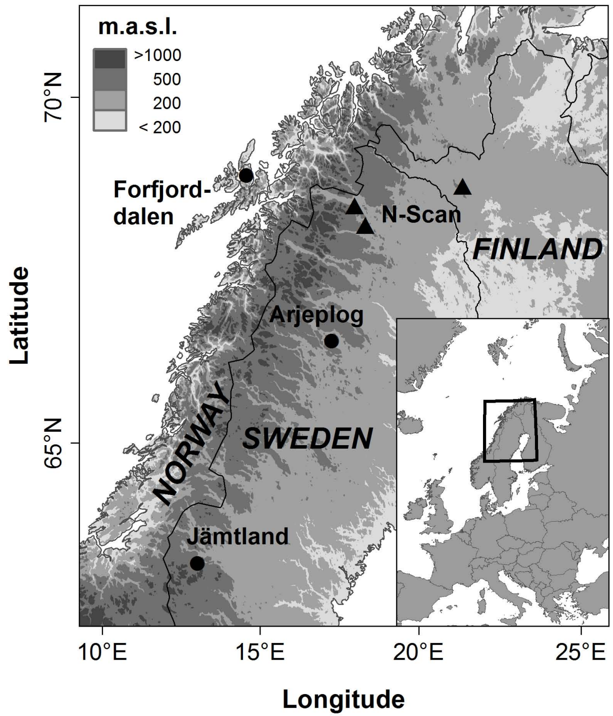

Fig. 3. Filled circles are the separate sites Arjeplog produced for this study, Jämtland and Forfjorddalen. Filled triangles are the modern part of the composite chronology N-Scan. Jämtland, Forfjorddalen and N-Scan are used as reference chronologies in this study.

CPD
9, 5227–5261, 2013

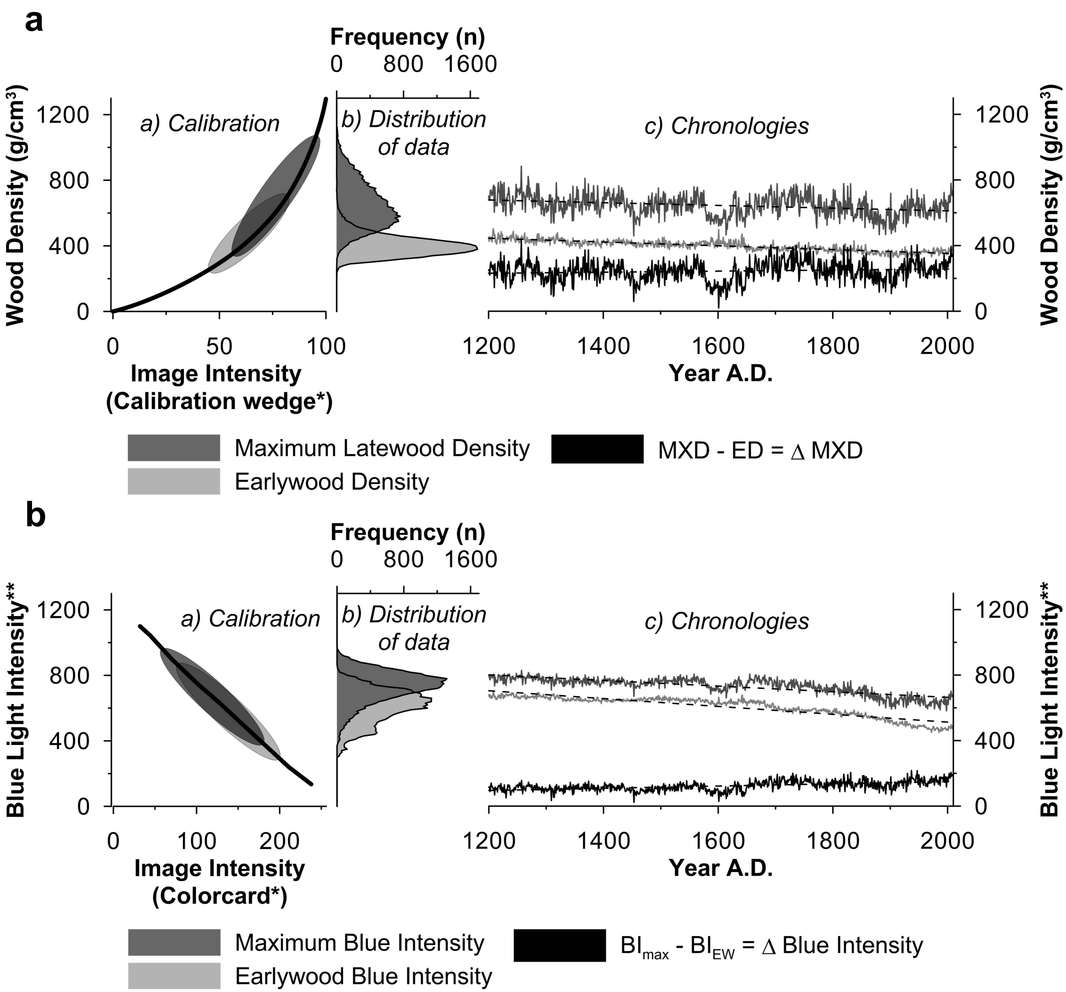

CPD
9, 5227–5261, 2013

Is Blue Intensity ready to replace Maximum Latewood Density?

J. A. Björklund et al.

c

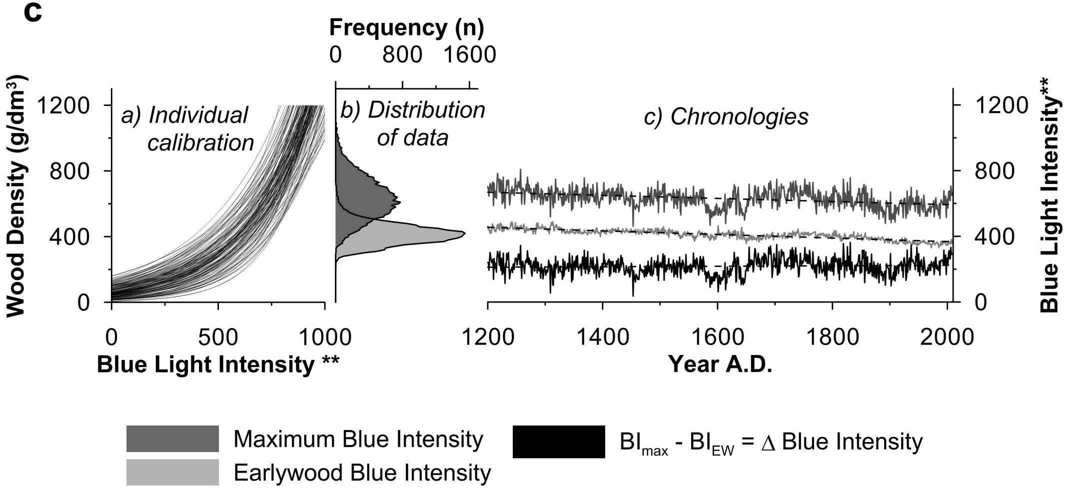

d

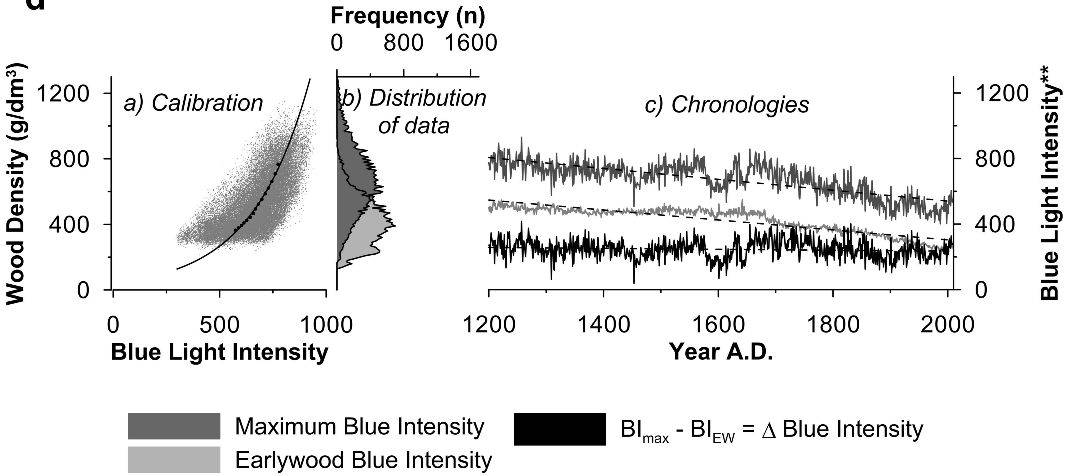

CPD
9, 5227–5261, 2013

Is Blue Intensity ready to replace Maximum Latewood Density?

J. A. Björklund et al.

Title Page
Abstract | Introduction
Conclusions | References
Tables | Figures
◀| |▶
◀ ▶
Back | Close
Full Screen / Esc
Printer-friendly Version
Interactive Discussion

Fig. 4. Left panel description: **(a)** calibration function based on measurements of X-Ray measurements of the standard, cellulose acetate calibration wedge, where MXD and ED values are schematically distributed along the function to visualise the resulting spread per grey level image intensity. **(b)** Inverted linear color calibration (not density calibration) of Blue Light Intensities to a standard color calibration target IT8/7. **(c)** Exponential functions that describe the relationship between wood density derived from ITRAX xray machine and the optical scanner on core level. **(d)** All raw data, X-Ray versus scans, are plotted together as one dataset against the other. The X-Ray dataset was sorted from low to high values and corresponding blue intensity values. A running mean of the two datasets were calculated for every 5000 data points with an overlap of 2500 data points, see black dots. These new running mean points were then regressed against one another and an OLS exponential function was calculated and used for calibration of the entire blue intensity dataset. Mid panel is histograms, distributions of the data points after calibration. In the right panels are mean chronologies for earlywood maximum latewood and also the Δ parameter.

CPD
9, 5227–5261, 2013

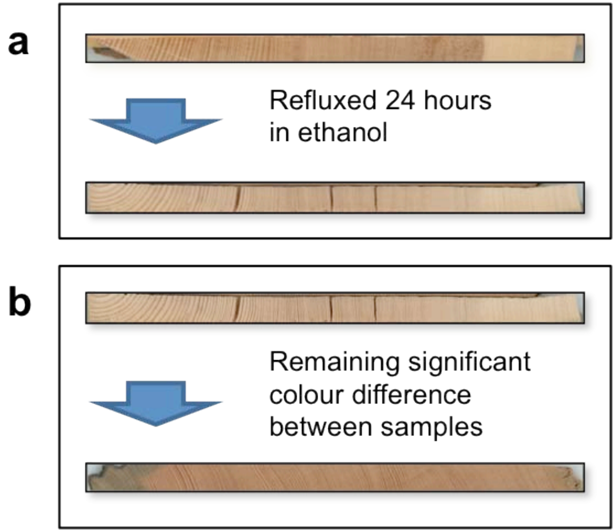

Fig. 5. (a) Photo of a living tree sample before and after alcohol soxhlet exctraction. **(b)** Example of two cores one living tree sample and one snag sample, dead since around 1650, death date unknown due to loss of sapwood.

CPD
9, 5227–5261, 2013

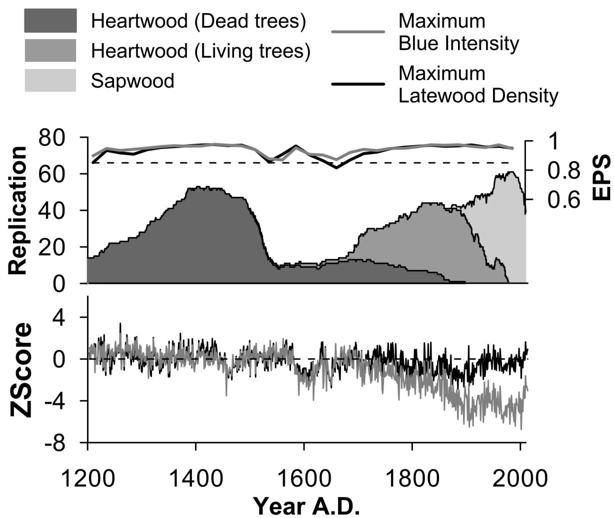

Fig. 6. MXD and BI_{max} chronologies with sample depth and expressed population signal (EPS). Replication is resolved into heartwood from snag material and heartwood from living trees and sapwood, almost exclusively from living trees.

CPD
9, 5227–5261, 2013

CPD
9, 5227–5261, 2013

Is Blue Intensity ready to replace Maximum Latewood Density?

J. A. Björklund et al.

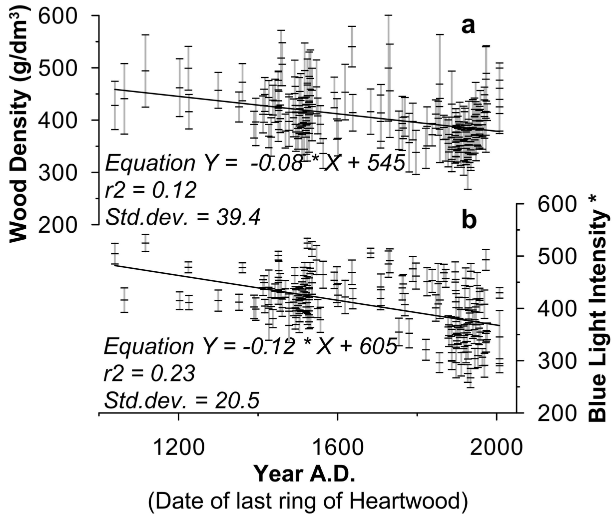

Fig. 7. (a) Combined MXD and ED mean and standard deviation regressed against date of last heartwood ring, with linear regression line. **(b)** Combined BI_{max} BI_{EW} mean and standard deviation regressed against date of last heartwood ring, with linear regression line.

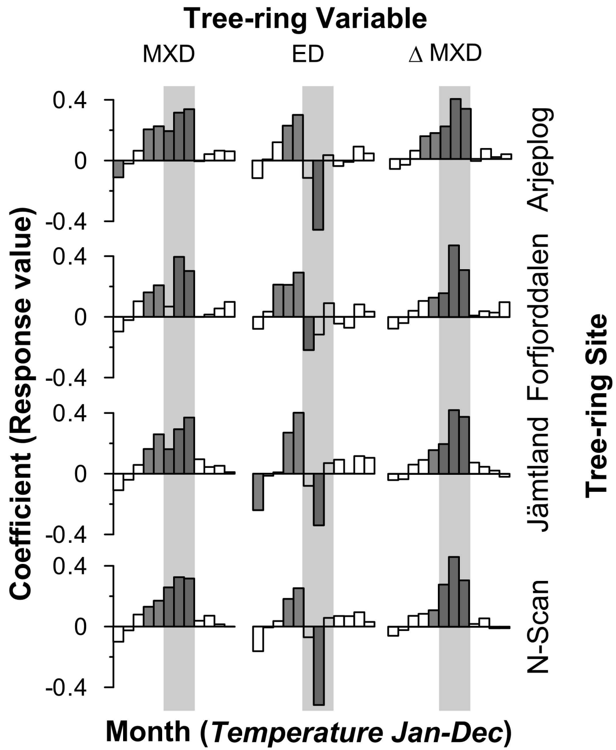

Fig. 8. Monthly temperature forcing upon different density parameter chronologies from Arjeplog Forfjorddalen, Jämtland and Finland N-Scan.

CPD

9, 5227–5261, 2013

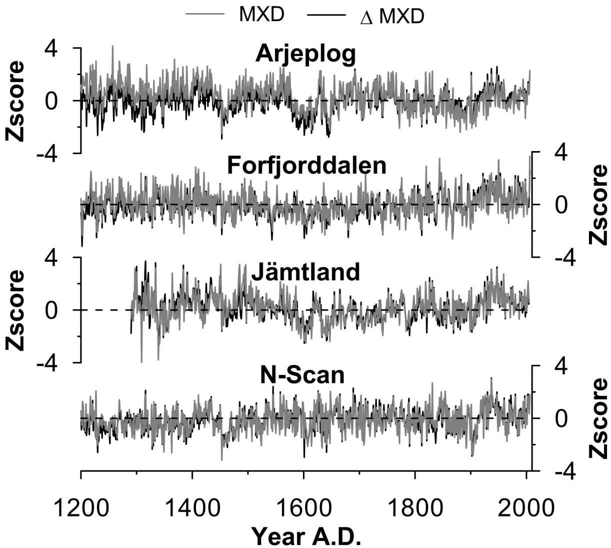

Fig. 9. MXD chronologies in grey plotted together with ΔMXD chronologies.

CPD
9, 5227–5261, 2013

Is Blue Intensity ready to replace Maximum Latewood Density?

J. A. Björklund et al.

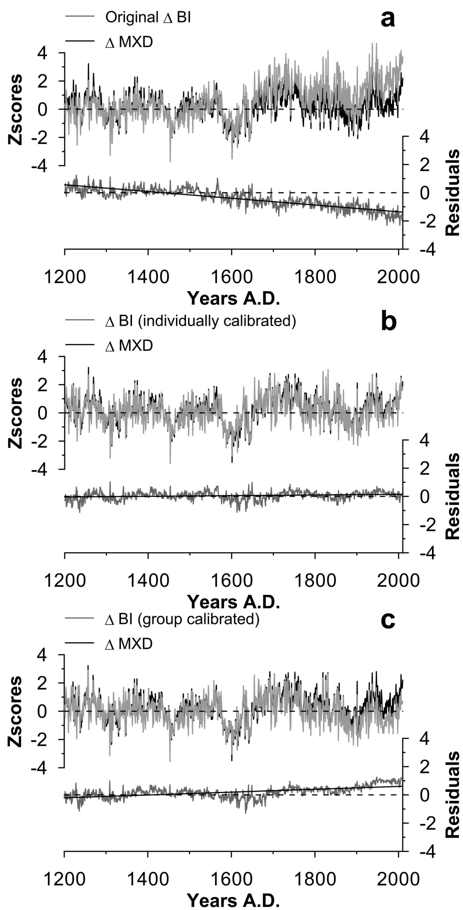

Fig. 10. ΔMXD plotted against **(a)** ΔBI, non-calibrated, **(b)** ΔBI, individually calibrated. **(c)** ΔBI, calibrated as a group, together with residuals.

CPD
9, 5227–5261, 2013

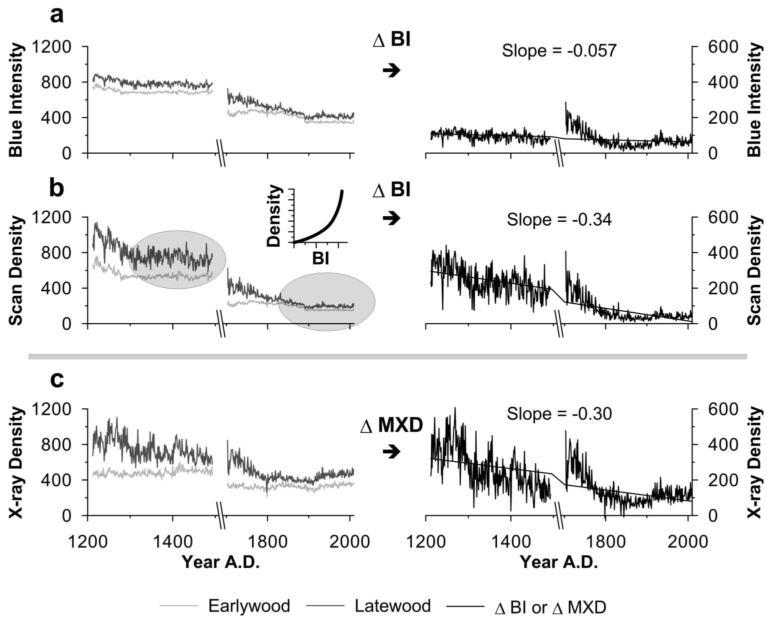

Fig. 11. The Diagram is made with the two real samples ARPS2011 and ARPS1212. Left panels: BI_{max} and BI_{EW} or MXD and ED, right panel: ΔBI or ΔMXD with slope between the two series. **(a)** Non-calibrated Blue intensity. **(b)** blue intensity calibrated as group into density, see small diagram in left panel, grey shaded circles highlight the variance compression and inflation that will result from using one calibration function when modern series on average have a lower mean brightness. **(c)** X-Ray density.

CPD
9, 5227–5261, 2013

Is Blue Intensity ready to replace Maximum Latewood Density?

J. A. Björklund et al.

Title Page
Abstract | Introduction
Conclusions | References
Tables | Figures
◀| |▶
◀ ▶
Back | Close
Full Screen / Esc
Printer-friendly Version
Interactive Discussion